
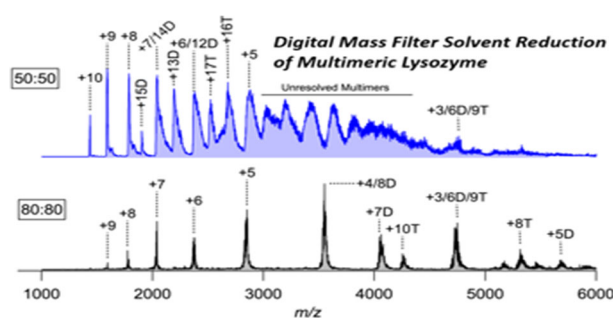


RESEARCH ARTICLE

Using Digital Waveforms to Mitigate Solvent Clustering During Mass Filter Analysis of Proteins

Bojana Opačić, Nathan M. Hoffman, Zachary P. Gotlib, Brian H. Clowers, Peter T. A. Reilly 

Department of Chemistry, Washington State University, Pullman, WA, USA



Abstract. With advances in the precision of digital electronics, waveform generation technology has progressed to a state that enables the creation of m/z filters that are purely digitally driven. These advances present new methods of performing mass analyses that provide information from a chemical system that are inherently difficult to achieve by other means. One notable characteristic of digitally driven mass filters is the capacity to transmit ions at m/z ratios that vastly exceed

the capabilities of traditional resonant systems. However, the capacity to probe ion m/z ratios that span multiple orders of magnitudes across multiple orders of magnitude presents a new set of issues requiring a solution. In the present work, when probing multiply charged protein species beyond m/z 2000 using a gentle atmospheric pressure interface, the presence of solvent adducts and poorly resolved multimers can severely degrade spectral fidelity. Increasing energy imparted into a target ion population is one approach minimizing these clusters; however, the use of digital waveform technology provides an alternative that maximizes ion transport efficiency and simultaneously minimizes solvent clustering. In addition to the frequency of the applied waveform, digital manipulation also provides control over the duty cycle of the target waveform. This work examines the conditions and approach leading to optimal digital waveform operation to minimize solvent clustering.

Keywords: Digital waveform technology, Digital mass filter, Protein mass analysis

Received: 16 April 2018/Revised: 1 June 2018/Accepted: 12 June 2018/Published Online: 9 July 2018

Introduction

The idea of using digital waveforms for mass filter analysis is attributed to Richards ca 1973 [1]. Unfortunately, the technology at the time to support digital waveform-based mass filter analysis could not really compete and overtake the already established sinusoidal technology. With the advent of direct digital synthesis (DDS), high voltage field effect transistors (HV-FET) and field programmable gate arrays (FPGA) in the 1990s, the technology to enable digital waveform-based mass analysis became available. Digital waveform technology (DWT) was first used to create a square wave-driven 3D ion trap by Shimadzu and introduced in 2001 [2]. Over the next 5 years, Shimadzu developed digital ion trap technology [3–6];

however, a commercial product was never produced. Though digital in nature, the approach and specific technology employed did not allow the square wave-driven ion trap to outperform its sinusoidal waveform technology (SWT) driven counterpart. Presumably, SWT traps were too entrenched in the market and the technology was too established for the square wave trap venture to be profitable.

Nonetheless, DWT had three notable theoretical advantages compared to SWT that remained unexplored. The first is the high frequency resolution over an extremely wide band that is available through DDS that enables a broad range of m/z to be probed with a single system [7]. Next is the ability to change the radial [8–10] and axial [11] stability of the ions on demand by changing the waveform duty cycle. The third, and perhaps most subtle capability enabled by DWT, is the agility of the waveform generation system. Waveforms can be changed instantaneously and then changed again with the only limitation

being the speed at which the waveform parameters may be transferred and registered on the DDS hardware. To be clear, the speed of the second change is what we refer to as agility [12]. The agility of the current waveform technology used in this work allows changes to be accomplished within one waveform cycle and allows the user to probe the impact of differing rates of excitation of the ions. This provides noticeable advantages with respect to ion excitation [8], isolation [13] and even mass analysis [14].

To ease the implementation and adoption of DWT, careful control of the duty cycle (i.e., the ratio of the high and low states of the waveform) supported the development of a digitally controlled mass filter [15, 16]. Historically, the method for generating rectangular waves was based on using DDS to create a frequency variable clock to operate digital counters. Using this approach, the duty cycle resolution was inherently limited by the integer number of clock cycle counts that created the rectangular wave. Despite the limitation of this generation method, the concept of using the duty cycle to create a narrowed mass window was first demonstrated by creating a crude mass filter to analyze IgG [17] and later, that same year, the duty cycle was used by Shimadzu to isolate charge states of cytochrome c. [18] Counter based rectangular WFG was also used in combination with frequency hopping to produce a narrow window of masses isolated within a linear ion guide. [13] This process was good enough to produce a credible, albeit slow, mass filter.

More recently, our group reported a comparator based method of rectangular waveform generation that provides superior duty cycle resolution compared to the initial reports limited by integer multiples of the waveform clock. [15, 16] Presently, the rectangular wave is created by comparing the highly accurate DDS sine wave output with a potential provided by an 18-bit digital to analog converter (DAC). The waveform duty cycle changes precisely with the change in the DAC output. This method provides sufficient duty cycle resolution to create purely digital mass filters and provides new methods of trapping and mass analysis.

Digitally driven mass filters extend the mass range beyond the currently available technology. With this increase in range, lower charge states of proteins and multimers are easily observed. These species tend to bind solvent better than higher charge state ions presumably because they are less denatured by greater charge-charge interactions. In this manuscript, we demonstrate a combination of digital ion trapping and mass filter methods that can be used to greatly minimize the presence of solvent adducts during the mass filter analysis of intact proteins using standard quadrupole rods.

Experimental

In this work lysozyme was used to demonstrate mass filter analysis of intact proteins. It was purchased from Sigma Aldrich company (St. Louis, MO) and used without further purification. 50% methanol/ 50% water (both HPLC grade and both from Fisher Chemical, Waltham MA) was used dissolve to dissolve the lysozyme and produce a 6 μM solution. No acid was added to the solution in order to shift the mass distribution to lower charge states. The instrument used in this effort is depicted in Fig. 1. The sample was introduced by electrospray ionization using the commercial fused silica capillary $30 \pm 2 \mu\text{M}$ tip (New Objective Co.) with an applied potential of +2600 V relative to the pinhole inlet. Sample solutions were pneumatically pushed through the capillary at 1 psig. Ions enter the instrument through a 300 μM diameter thin plate orifice and expand within a digitally-operated ion funnel operated at 500 kHz and 48Vp-p with a -50 VDC potential across the funnel in a differentially pumped chamber at approximately 1.3 Torr. [19] The AC and DC fields of the funnel collimate and push the ions toward the exit orifice and into a digitally-operated ion guide at 10 mTorr.

The guide is driven by a pair of high voltage waveforms created by two separate pulsers, one for each electrode pair. The pulsers are essentially high voltage switches that toggle the output from high voltage DC power supplies. The power supplies were maintained at a constant difference of 300 V. The duty cycle of a waveform is defined by the percentage of the cycle that the waveform is in the high state. To achieve trapping and m/z filtering, the waveforms applied to each pair of electrodes of a quadrupole guide or filter are defined by a pair of duty cycles, the percentages of time the waveforms are in the high states. For axial trapping waveforms, the duty cycle values add to less than 100%, whereas duty cycle values for ejection add to greater than 100%. In these experiments, the trapping duty cycle was set to 32/32 and the trapping time was held constant at 68 ms. The 32/32 axial trapping waveforms are depicted in Fig. 2 to illustrate the waveform nomenclature used. The values t_n define the four period fractions of constant potential during the waveform. The ejection duty cycles were changed from 50/50 to 80/80 in increments of 10, while maintaining a constant ejection axis potential of 1 V. To maintain the constant ejection axis potential with the changing duty

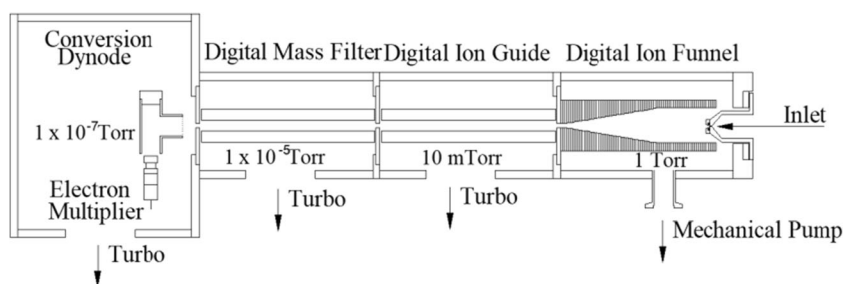


Figure 1. Instrumental layout detailing a stacked ring ion funnel which transitions into an ion guide which itself is digitally driven. The first ion guide can also serve as an ion trapping device prior to mass filtering in the second quadrupole

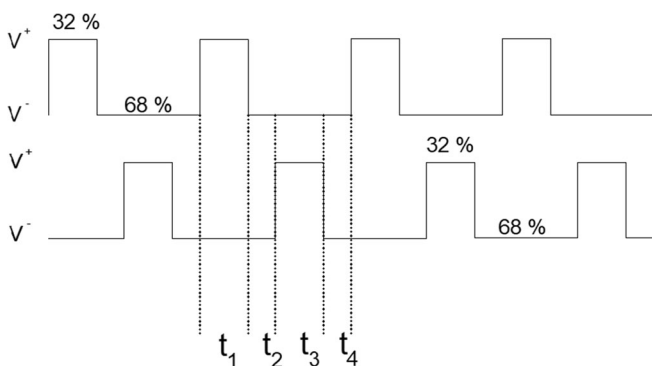


Figure 2. An example of a 32/32 comparator-generated waveform that defines the constant voltage segments of the waveform, t_1 , t_2 , t_3 , and t_4 . V^+ and V^- are the power supply voltages

cycle, the pulser power supply voltages were changed to compensate for the duty cycle-induced axis potential shift. The trapping axis potential changes while at a constant trapping duty cycle because of the change in the pulser power supply potential. The time-weighted average of the DC axis potential for trapping or ejection is given by:

$$V_{\text{axis}} = \sum_n t_n \left(\frac{V_{1,n} + V_{2,n}}{2} \right), \quad (1)$$

where $V_{1,n}$ is the voltage of electrode pair 1 during the n th constant voltage segment of the rectangular waveform pair. $V_{2,n}$ is the voltage on electrode pair 2 during the n th constant voltage segment of the waveforms (see Fig. 2 for the definition of the constant voltage time segments). This equation defines the DC axis potential for any rectangular waveform pair when the Mathieu parameter $a = 0$. The digital mass filter (DMF) had zero axis potential and the duty cycle applied to it was 61.1/38.9. The ions exiting the DMF impacted into the conversion dynode at approximately -7000 V. The converted charges were detected with an electron multiplier. The amplifier gain was set to 1×10^8 .

Results and Discussion

There is a limited mass range for SWT-driven analyzers that is defined by the frequency of the resonantly tuned rf driving circuit. For commercial triple quadrupole mass spectrometers, 2000 to 3000 mass units are the general upper mass limit because they scan the voltage at fixed frequency. To broaden the mass range of SWT-driven instruments, multiple resonantly tuned rf driving circuits (i.e., multiple WFGs) would be required to increase the range by an order of magnitude. Implementation of multiple driving circuits is difficult to orchestrate and more expensive. On the other hand, because DWT scans the frequency while fixing the voltage, the m/z that can be observed is limited only by the ionization source and transfer optics. In fact, digital mass filter analysis (albeit poorly resolved because of the limitation of the WFG at the time) has

been demonstrated to $m/z 1 \times 10^6$ and the range was only limited by the detector sensitivity [17].

In this work, we present the digital mass filter spectra of lysozyme taken as a function of duty cycle trapping axis potential and the same ejection axis potential V_{axis} or beam voltage into an awaiting digital mass filter. The ions were axially collected and trapped in the first quadrupole for 68 ms with a broadband 32/32 trapping duty cycle waveform and subsequently axially ejected into the mass filter with varying ejection duty cycles. For reference, Fig. 2 illustrates a comparator-generated 32/32 waveform. The axial beam energy at ejection was maintained at 1 V by adjusting the DC power supplies (V^+ and V^-) that drive the high voltage pulsers. Because the axis potential of the mass filter was maintained at 0 V, the beam energy (voltage) at ejection is defined by the time-weighted average of the DC axis potential calculated in Eq. (1). Figure 3 presents the axis potentials during axial trapping of the ions in the first quadrupole and subsequent ejection of the trapped ions into the digital mass filter. Because the axis potential at ejection is maintained at 1 V the power supply potentials, V^+ and V^- have to be adjusted to offset the change made by changing the ejection duty cycle. These power supply voltage changes also change the axis potential during trapping in the manner described by the above equation. The axis potentials and corresponding power supply voltages are shown in Fig. 3. Figure 2 shows an example of comparator-generated waveforms to define the constant voltage segments of the waveforms. The t_1 and t_3 segments V_{1n} and V_{3n} are V^+ and V^- and vice versa, while during t_2 and t_4 , they are at V^- to create axial trapping waveform conditions (they would be at V^+ during axial ejection).

Figure 4 presents the spectra of lysozyme injected into the digital mass filter with (a) 50/50, (b) 60/60, (c) 70/70, and (d) 80/80 duty cycle and 1 V beam energy. The axis potentials during the 68-ms trapping period are (a) -53 , (b) -83 , (c) -113 , and (d) -143 V. The processes of trapping and ejection represent two relatively large changes in the axis potential for each presented spectrum. The 50/50 duty cycle ejection

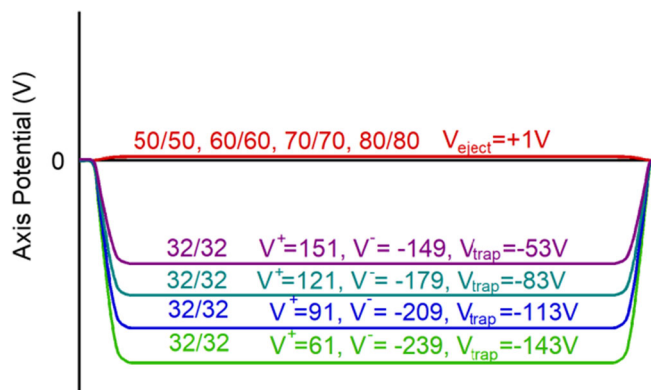


Figure 3. A plot of the axis potentials for trapping and ejection for 50/50, 60/60, 70/70, and 80/80 duty cycle ejection. A 32/32 trapping duty cycle was used yielding -53 , -83 , -113 , and -143 V axis potentials during collection, respectively

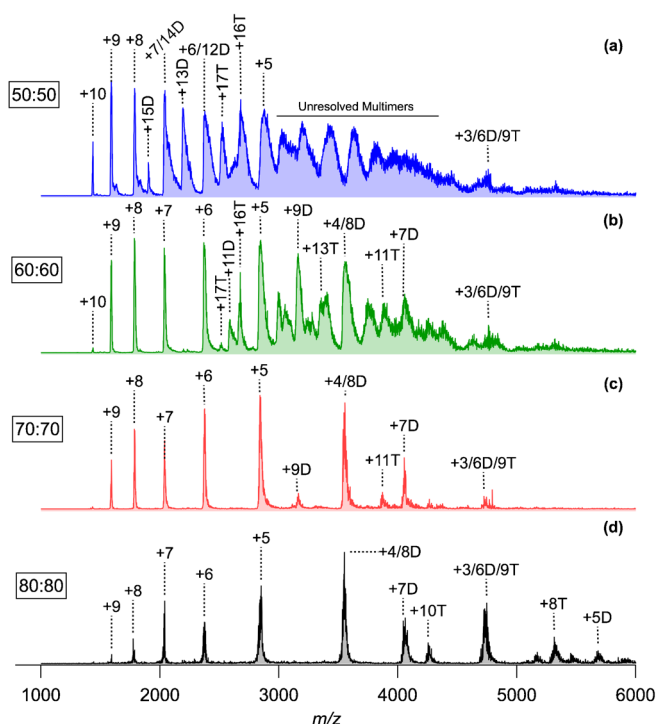


Figure 4. Lysozyme spectra at (a) 50/50, (b) 60/60, (c) 70/70, and (d) 80/80 duty cycle eject waveform with 1 V beam energy. Changing the trapping well depth with increasing ejection duty cycle decreases solvent adducts

spectrum shown in Fig. 4(a) presents clear formation of solvent adducts with the intact protein ions as evidenced by the broadening of the mass peaks. Solvent adduction is clearly charge state dependent because the lower m/z (higher charge) ions demonstrate much narrower peak widths.

The electrosprayed solution was 6 μM in a denaturing 50% water 50% ethanol solution with no acid added. These ESI conditions were selected to yield lower charge state (higher m/z) distributions. The increased concentration of the working solution was chosen to promote the formation of multimeric species. The charge states have been labeled for each peak as were the positions of the multimer ions up trimer ions. Although there is evidence of higher order multimers as revealed by the unlabeled peaks in the spectra. Only the dimer and trimer ion positions were labeled with “D” and “T,” respectively. Multimeric species are prominently observed in the spectra displayed in Figs. 4 and 5 presumably because no acid was added to the electrosprayed solution. A 6 μM solution of lysozyme does not normally yield such large concentrations of multimers when acid is added.

It is also worth noting that the presence and distribution of such multimers and charge states were manipulated using DWT technology in a fashion unique to this mode of mass filtering. As the duty cycle of the ejection and the depth of the axial trapping well increases in the spectral series, the presence of solvent adducts decreases as does the larger charge state multimers. Moreover, there appears to be a shift to lower

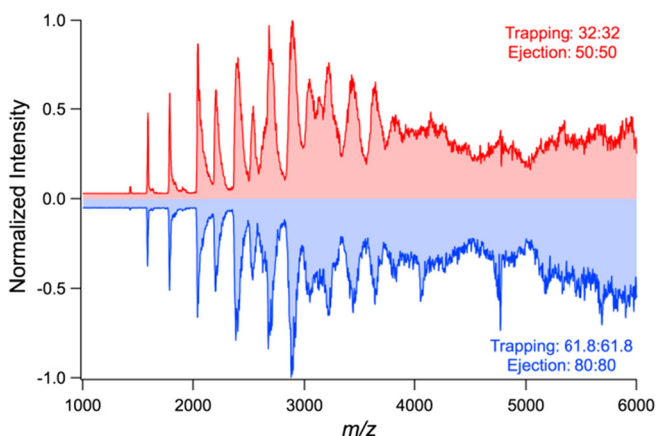


Figure 5. Lysozyme digital mass filter spectrum with (a) 61.8/61.8 trapping and 80/80 ejection duty cycle and (b) 32/32 trapping and 50/50 ejection duty cycle. Both feature a -54 V trapping and a 1 V ejection potential and are essentially identical

charge state multimers as evidenced by the emergence of the band of peaks above m/z 5000 for the 80/80 duty cycle spectrum. The unlabeled peaks in the 80/80 ejection spectrum do not fit within the trimer, dimer, or monomer ion series. Currently, we suspect that these peaks arise from higher order multimers including tetramers and even possibly pentamers. All four spectra in Fig. 4 are on the same scale and the collection time was 68 ms for each. Therefore, the results above m/z 5000 suggest charge stripping of higher order multimer ions while multimer ion cleavage is most likely creating the changes in the ion distributions.

Clearly, the trapping and ejection processes are heating the ions, the deeper axial trapping wells yielding greater thermal excitation. Large changes in axis potential in moving into or out of a gas-filled quadrupole induce collisional heating. This trapping well-induced heating can easily be prevented merely by changing the trapping duty cycle. For example, the trapping duty cycle during the 80/80 ejection scan can be changed to 61.8/61.8 to yield the same -53 V axial potential observed in the 50/50 ejection scan in Fig. 4. Consequently, even though these power supply potentials and trapping and ejection duty cycles are very different, the spectra should be identical because they both have a -53 V axis potential during trapping and a 1 V axis potential during ejection. This hypothesis was tested with the lysozyme spectra presented in Fig. 5. The spectra were taken in tandem, (a) presents a 61.8/61.8 trapping and 80/80 ejection duty cycle and (b) presents a 32/32 trapping and 50/50 ejection duty cycle. Both feature an approximately -53 V trapping and a 1 V ejection potential. Given the positive comparison, our supposition that the change in the axis potentials drive the thermal excitation that yield the redistribution of the ions appears to be correct.

This work highlights the capacity of DWT to manipulated large ions and controls the degree of multimer formation. Specifically, our data show that the excitation of non-covalently bound multimeric protein ions can be tightly

controlled to strip the ions of solvent adducts while maintaining the noncovalent binding of the proteins. While it is certainly true that the SWT axis potential can be shifted to cause thermal heating of the ions, it is the ability to perform this operation with the agility and precision of DWT trapping followed by controlled rapid ejection that sets it apart. DWT provides more options as well as speed and precision for manipulating the ions while vastly increasing the mass range. Moreover, we have previously shown that there are other options for exciting ions trapped in a linear quadrupole [8]. It has again been demonstrated that menu of options for DWT manipulation of ions exceeds that offered by SWT.

Conclusion

The work shown here demonstrates the capabilities of DWT to manipulate and analyze intact proteins and their noncovalent multimeric ions. DWT was precisely used to excite the protein and cluster ions to remove solvent adducts while maintaining the integrity of the multimeric ions. Consequently, intact proteins and noncovalent clusters can be mass analyzed with a DWT-based mass filter. Though the DWT-based spectra observed here double the range of commercial triple quadrupole mass spectrometers, the real mass range of this analyzer has yet to be demonstrated. According to theory, the range should be limited by ion source conditions and the range of the detector which presently approaches 1 MDa [17].

Funding Information

This work was supported by the National Science Foundation Award No. 1352780.

References

1. Richards, J.A., Huey, R.M., Hiller, J.: A new operating mode for the quadrupole mass filter. *Int. J. Mass Spectrom. Ion Phys.* **12**, 317–339 (1973)
2. Ding, L., Gelstrop, A., Nutall, J., Kumashiro, S.: Rectangular Wave Quadrupole Field and Digital Q(IT)MS Technology. in 49th American Society for Mass Spectrometry Conference on Mass Spectrometry and Applied Topics. Chicago, Illinois (2001)
3. Ding, L., Brancia, F.L.: Electron capture dissociation in a digital ion trap mass spectrometer. *Anal. Chem.* **78**, 1995–2000 (2006)
4. Ding, L., Kumashiro, S.: Ion motion in the rectangular wave quadrupole field and digital operation mode of a quadrupole ion trap mass spectrometer. *Rapid Commun. Mass Spectrom.* **20**, 3–8 (2006)
5. Ding, L., Sudakov, M., Brancia, F.L., Giles, R., Kumashiro, S.: A digital ion trap mass spectrometer coupled with atmospheric pressure ion sources. *J. Mass Spectrom.* **39**, 471–484 (2004)
6. Ding, L., Sudakov, M., Kumashiro, S.: A simulation study of the digital ion trap mass spectrometer. *Int. J. Mass Spectrom.* **221**, 117–138 (2002)
7. Brandon, D.: Direct digital synthesizers in clocking applications time jitter in direct digital synthesizer-based clocking systems. *Analog Devices Appl. Notes.* 1–8 (2006). http://www.analog.com/media/en/technical-documentation/applicationnotes/475354741144165304775709740692131461831AN823_0.pdf
8. Brabeck, G.F., Chen, H., Hoffman, N.M., Wang, L., Reilly, P.T.A.: Development of MSn in digitally operated linear ion guides. *Anal. Chem.* **86**, 7757–7763 (2014)
9. Brabeck, G.F., Reilly, P.T.A.: Mapping ion stability in digitally driven ion traps and guides. *Int. J. Mass Spectrom.* **364**, 1–8 (2014)
10. Brabeck, G.F., Reilly, P.T.A.: Computational analysis of non-traditional waveform quadrupole mass filters. *J. Am. Soc. Mass Spectrom.* **27**, 1122–1127 (2016)
11. Lee, J., Marino, M.A., Koizumi, H., Reilly, P.T.A.: Simulation of duty cycle-based trapping and ejection of massive ions using linear digital quadrupoles: the enabling technology for high resolution time-of-flight mass spectrometry in the ultra high mass range. *Int. J. Mass Spectrom.* **304**, 36–40 (2011)
12. Hoffman, N.M., Gotlib, Z.P., Opačić, B., Huntley, A.P., Moon, A.M., Donahoe, K.E.G., Brabeck, G.F., Reilly, P.T.A.: Digital waveform technology and the next generation of mass spectrometers. *J. Am. Soc. Mass Spectrom.* **29**, 331–341 (2018)
13. Gotlib, Z.P., Brabeck, G.F., Reilly, P.T.: Methodology and characterization of isolation and preconcentration in a gas-filled digital linear ion guide. *Anal. Chem.* **89**, 4287–4293 (2017)
14. Donahoe, K.E.G., Moon, A. M., Gotlib, Z. P., Hoffman, N. M., Reilly, P. T. A.: Digital Mass Scanning Techniques without Dipolar Auxiliary Waveforms. In 65th American Society for Mass Spectrometry Conference. Indianapolis, IN, (2017)
15. Hoffman, N.M., Gotlib, Z.P., Opačić, B., Clowers, B.H., Reilly, P.T.A.: A comparison based digital waveform generator for high resolution duty cycle. Review of scientific instruments. Under Review (2017)
16. Hoffman, N.M., Gotlib, Z. P., Opačić, B., Clowers, B.H., Reilly, P.T.A.: Generation of Digital Waveforms with High Resolution Duty Cycle. In 65th American Society for Mass Spectrometry Conference on Mass Spectrometry and Allied Topics. Indianapolis, IN, (2017)
17. Koizumi, H., Whitten, W.B., Reilly, P.T.A.: Controlling the expansion into vacuum—the enabling technology for trapping atmosphere-sampled particulate ions. *J. Am. Soc. Mass Spectrom.* **21**, 242–248 (2010)
18. Brancia, F.L., McCullough, B., Entwistle, A., Grossmann, J.G., Ding, L.: Digital asymmetric waveform isolation (DAWI) in a digital linear ion trap. *J. Am. Soc. Mass Spectrom.* **21**, 1530–1533 (2010)
19. Hoffman, N.M., Opačić, B., Reilly, P.T.A.: Note: an inexpensive square waveform ion funnel driver. *Rev. Sci. Instrum.* **88**, 3 (2017)